Communications

Lithium Niobate Microtubes within Ordered Macroporous Silicon by Templated Thermolysis of a Single Source Precursor

Lili Zhao,† Martin Steinhart,*,† Maekele Yosef,‡ Sung Kyun Lee,† Torsten Geppert,† Eckhard Pippel,† Roland Scholz,† Ulrich Gösele,† and Sabine Schlecht‡

Max Planck Institute of Microstructure Physics, Weinberg 2, 06120 Halle, Germany, and Department of Chemistry, Philipps University, Hans-Meerwein-Strasse, 35032 Marburg, Germany

Received September 12, 2004
Revised Manuscript Received November 18, 2004

Lithium niobate ($LiNbO_3$) has been used for all-optical wavelength conversion[1] and ultrafast optical signal processing[2−5] because of its outstandingly rapid nonlinear optical response behavior, low switching power, and broad conversion bandwidth. Periodically poled photonic crystals[6] and inverse artificial opals made of $LiNbO_3$[7] have been reported. Ordered macroporous silicon (Si)[8−10] is an extensively investigated two-dimensional photonic band gap material. Here we report on the preparation of hybrid systems consisting of $LiNbO_3$ and macroporous Si. Such composites are of considerable interest because of the integration of $LiNbO_3$ into silicon photonics. For instance, the band gap of macroporous Si could be tuned by poling $LiNbO_3$ and thus changing its dielectric constant. Moreover, we investigated whether released $LiNbO_3$ tubes are accessible using macroporous Si as a sacrificial template. We have adapted a methodology involving the use of porous matrixes as molds, as investigated by Martin[11−13] and others.[14−20] We

Scheme 1. Molecular Structure of Lithium[Tetraethoxy(1-phenyl-1,3-butanedione)Niobate]

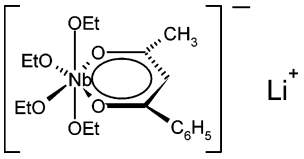

dropped a 5% solution of lithium [tetraethoxy(1-phenyl-1,3-butanedione)niobate] (Scheme 1) in ethanol at ambient conditions on macroporous Si with a pore diameter, D_p, of 1 μm. The synthesis and the properties of this single-source precursor for $LiNbO_3$ are described elsewhere.[21] The Si substrate into which the macropores were etched was a single-crystalline (100)-oriented wafer. We removed the residual liquid from the template surface. As the solvent evaporates, a layer of adsorbed molecules remains at the pore walls, which can be converted to the target compound by thermolysis. This procedure may be repeated once or several times. The conversion to crystalline $LiNbO_3$ was performed by annealing the wetted templates at 550, 650, and 750 °C, respectively, for 5 h. Then, the samples were cooled to room temperature at a rate of 2 K/min. Note that all these steps were performed under an argon atmosphere. The templates may be etched with 30 wt % aqueous KOH either partially at room temperature or completely at 70 °C.

Figure 1 represents $LiNbO_3$ tubes annealed at 550 °C, prepared by two successive wetting−crystallization−cooling cycles. Figure 1a shows a scanning electron microscopy (SEM) image of the openings of $LiNbO_3$ tubes partially embedded in the template. Their wall thickness is approximately 30 nm. A completely released $LiNbO_3$ tube is depicted in Figure 1b. Its aspect ratio (length/diameter) equals 100. The inset (top right of Figure 1b) shows its open end at higher magnification. Figure 1c is a bright field transmission electron microscopy (TEM) image, and Figure 1d is the corresponding dark field micrograph of a detail of a tube wall.

We performed X-ray diffraction (XRD) experiments in the reflection mode on aligned $LiNbO_3$ tubes located in the template pores. The samples were mounted in such a way that the long axes of the tubes were oriented parallel, and the template surface was perpendicular to the plane defined

* To whom correspondence should be addressed. E-mail: steinhart@mpi-halle.de.
† Max Planck Institute of Microstructure Physics.
‡ Philipps University.

(1) Magel, B. A.; Fejer, M. M.; Byer, R. L. *Appl. Phys. Lett.* **1990**, *56*, 108−110.
(2) Benner, A. F.; Jordan, H. F.; Heuring, V. P. *Opt. Eng.* **1991**, *30*, 1936−1941.
(3) Asobe, M.; Yokohama, I.; Itoh, H.; Kaino, T. *J. Opt. Lett.* **1997**, *22*, 274−276.
(4) Parameswaran, K. R.; Fujimura, M.; Chou, M. H.; Fejer, M. M. *IEEE Photon. Technol. Lett.* **2000**, *12*, 341−343.
(5) Kanter, G. S.; Kumar, P.; Parameswaran, K. R., Fejer, M. M. *IEEE Photon. Technol. Lett.* **2001**, *13*, 654−656.
(6) Berger, V. *Phys. Rev. Lett.* **1998**, *81*, 4136−4139.
(7) Wang, D. Y.; Caruso, F. *Adv. Mater.* **2003**, *15*, 205−210.
(8) Lehmann, V. *J. Electrochm. Soc.* **1993**, *140*, 2836−2843.
(9) Lehmann, V.; Föll, H. *J. Electrochem. Soc.* **1990**, *137*, 653−658.
(10) Birner, A.; Grüning, U.; Ottow, S.; Schneider, A.; Müller, F.; Lehmann, V.; Föll, H.; Gösele, U. *Phys. Status Solidi A* **1998**, *165*, 111−117.
(11) Martin, C. R. *Adv. Mater.* **1991**, *3*, 457−459.
(12) Martin, C. R. *Science* **1994**, *266*, 1961.
(13) Lakshmi, B.; Dorhout, P. K.; Martin, C. R. *Chem. Mater.* **1997**, *9*, 857−862.
(14) Steinhart, M.; Wendorff, J. H.; Greiner, A.; Wehrspohn, R. B.; Nielsch, K.; Schilling, J.; Choi, J.; Gösele, U. *Science* **2002**, *296*, 1997.
(15) Tian, M.; Wang, J.; Kurtz, J.; Mallouk, T. E.; Chan, M. H. W. *Nano Lett.* **2003**, *3*, 919−923.
(16) Liang, Z.; Susha, A. S.; Yu, A.; Caruso, F. *Adv. Mater.* **2003**, *15*, 1849−1853.
(17) Lahav, M.; Sehayek, T.; Vaskevich, A.; Rubinstein, I. *Angew. Chem., Int. Ed.* **2003**, *42*, 5576−5579.
(18) Steinhart, M.; Wehrspohn, R. B.; Gösele, U.; Wendorff, J. H. *Angew. Chem., Int. Ed.* **2004**, *43*, 1334−1344.
(19) Steinhart, M.; Jia, Z.; Schaper, A. K.; Wehrspohn, R. B.; Gösele, U.; Wendorff, J. H. *Adv. Mater.* **2003**, *15*, 706−709.
(20) Göring, P.; Pippel, E.; Hofmeister, H.; Wehrspohn, R. B.; Steinhart, M.; Gösele, U. *Nano Lett.* **2004**, *4*, 1121−1125.
(21) Hirano, S.; Takeichi, Y.; Sakamoto, W.; Yogo, T. *J. Cryst. Growth* **2002**, *237−239*, 2091−2097.

10.1021/cm0484302 CCC: $30.25
Published on Web 12/13/2004

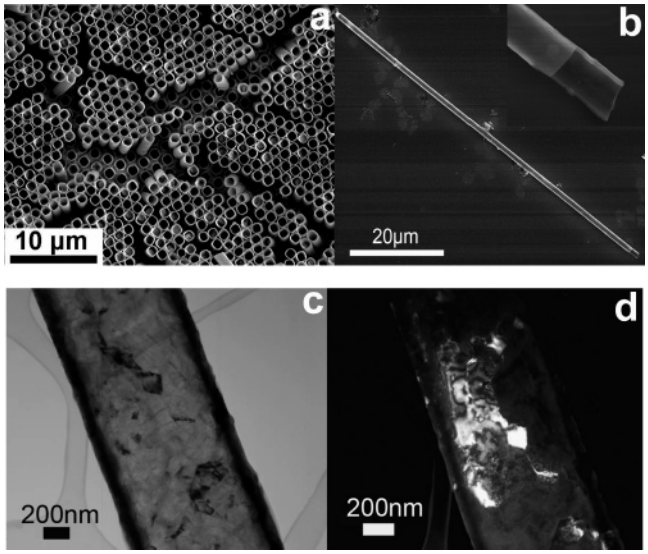

Figure 1. $LiNbO_3$ microtubes prepared by two successive wetting−crystallization−cooling cycles with an annealing temperature of 550 °C. SEM images of (a) openings of tubes attached to a partially removed template and (b) a released tube lying on a silicon substrate (inset: opening at higher magnification). (c) Bright-field and (d) dark-field TEM image of a tube wall.

by the incident beam and the detector. The samples may also be tilted by an angle Ψ around an axis defined by the intersection of the template surface and the plane of the incident and the scattered X-ray beams. Both the Ψ and Θ axes lie in the plane of the sample surface, enclosing a right angle (Scheme 2). All samples investigated showed the characteristic reflections of pure $LiNbO_3$ independent of the selected thermolysis temperature and the number of wetting−crystallization−cooling cycles.

Scheme 2. Setup Used for XRD Experiments[a]

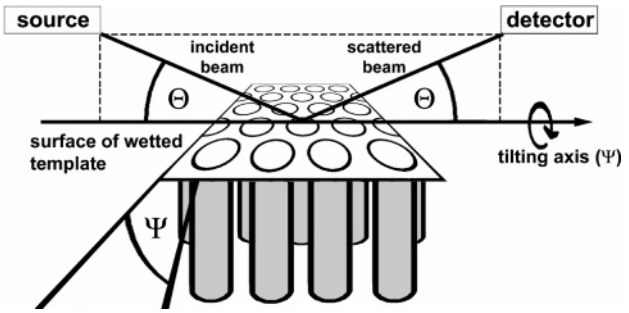

[a] For the Θ/2Θ scans the samples were placed in the device in such a way that the surfaces of the templates were oriented perpendicularly to the plane defined by the incident and scattered X-ray beams. The samples may also be tilted by an angle Ψ around an axis defined by the intersection of the template surface and the plane of the incident and the scattered X-ray beams.

Figure 2a displays the Θ/2Θ scan of $LiNbO_3$ tubes within macroporous Si, fabricated by two consecutive wetting−crystallization−cooling cycles performed at 650 °C and one further cycle at 750 °C, with Ψ adjusted to 0°. For the Θ/2Θ scan of the same sample represented in Figure 2b, however, we selected a Ψ value of 10°. Figure 2c shows for comparison a powder diffractogram of $LiNbO_3$ measured on randomly oriented crystallites prepared by milling a single crystal of the ferroelectric noncentrosymmetric modification (space group *R*3*c*), fabricated by the Czochralski method,

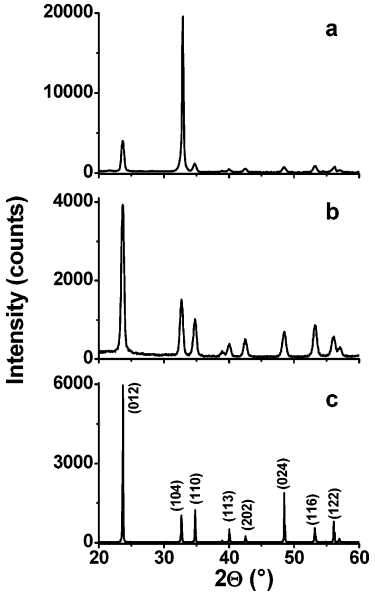

Figure 2. Θ/2Θ scans on aligned $LiNbO_3$ tubes within macroporous Si, prepared by two wetting−crystallization−cooling cycles at 650 °C and one further wetting−crystallization−cooling cycle at 750 °C: (a) Ψ = 0° and (b) Ψ = 10°. (c) Powder pattern of the ferroelectric noncentrosymmetric modification of $LiNbO_3$.

on a flat (100) Si wafer. The reflections were indexed according to JCPDS entry 78-0250. A conspicuous feature present in all diffractograms recorded with Ψ = 0°, independent of the annealing temperature and the number of wetting−crystallization−cooling cycles, is that the strongest peak appears at 2Θ = 32.8°. The corresponding XRD patterns of $LiNbO_3$/macroporous Si hybrid materials prepared by one wetting−crystallization−cooling cycle, and two consecutive wetting−crystallization−cooling cycles, respectively, at 550 °C are shown in the Supporting Information (Figure S1). At 2Θ = 32.8° the (104) reflection of $LiNbO_3$ and the (200) reflection of Si may coincide. The latter is a forbidden peak which only occurs when the Si lattice is distorted. Both XRD patterns displayed in Figure 2a and b show the characteristic reflections of pure $LiNbO_3$. The striking difference is, however, that the very strong peak at 32.8° is not present in Figure 2b, which is similar to the powder pattern (Figure 2c), particularly regarding the relative peak intensities of the (012) and (104) reflections. Tilting the samples by 10° around the Ψ axis moves the scattered intensity originating from the {k00} reflections of macroporous Si out of the coverage of the detector. Therefore, we ascribe the strong reflection at 2Θ = 32.8° occurring in the Θ/2Θ scans with Ψ adjusted to 0° predominantly to the (200) peak of Si. In the Θ/2Θ scan measured with Ψ adjusted to 10° the intensity in the corresponding 2Θ range exclusively originates from the (104) reflection of $LiNbO_3$.

It is well-known that thermal oxidation of macroporous Si imposes considerable mechanical stress on Si forming the pore walls.[22] However, solely annealing macroporous silicon under argon does not result in the occurrence of lattice distortions abrogating the extinction of the (200) reflection (Supporting Information, Figure S2). Hence, the Si lattice

(22) Ottow, S.; Lehmann, V.; Föll, H. *J. Electrochem. Soc.* **1996**, *143*, 385−390.

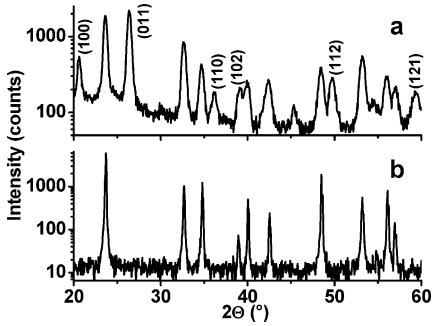

Figure 3. Θ/2Θ scan of aligned $LiNbO_3$ tubes within macroporous Si, prepared by two wetting−crystallization−cooling cycles at 650 °C under ambient conditions. The peaks that can be ascribed to quartz are denoted by the corresponding (*hkl*) values. (b) Powder pattern of the ferroelectric noncentrosymmetric modification of $LiNbO_3$.

must have been distorted upon the conversion of the lithium [tetraethoxy(1-phenyl-1,3-butanedione)niobate] into $LiNbO_3$.

Figure 3 shows the Θ/2Θ scan of $LiNbO_3$ tubes within macroporous silicon, recorded with $\Psi = 10°$, after two wetting−crystallization−cooling cycles at 650 °C under ambient conditions. Besides the $LiNbO_3$ peaks, a second set of reflections occurs, which we ascribe to trigonal quartz (space group $P3_221$, according to JCPDS entry 85-0794). This result indicates that the nature of the interface between $LiNbO_3$ and the pore wall is influenced by the presence or absence of oxygen.

Following the approach reported here a material with rapid nonlinear optical response behavior, low switching power, and broad conversion bandwidth can be incorporated into a two-dimensional photonic crystal made of macroporous silicon. This may allow for switching the photonic band gap material by changing the polarization of $LiNbO_3$. Along with the possibility to generate specific functional defect structures by omitting pores at specific positions, microscaled building blocks for high-speed optical switching and wavelength conversion may be accessible. The presented synthetic methodology is furthermore a generic approach for the fabrication of one-dimensional nano- and microstructures that can be adapted to any other functional material for which a suitable precursor system exists.

Acknowledgment. We thank Dr. Petra Göring for additional XRD measurements and Yun Luo for fruitful discussions, as well as the Deutsche Forschungsgemeinschaft for funding in the framework of the priority program SPP 1165 "Nanowires and Nanotubes" (STE 1127/2-1 and SCHL 529/2-1). S. Schlecht thanks the Fonds der Chemischen Industrie and the Dr. Otto Röhm-Gedächtnisstiftung for funding.

Supporting Information Available: $\theta/2\theta$ scans recorded with $\Psi = 0°$ on aligned $LiNbO_3$ tubes within macroporous Si prepared at 550 °C and powder pattern of the ferrolectric noncentrosymmetric modification of $LiNbO_3$ (Figure S1), and details of a $\theta/2\theta$ scan on (100) oriented macroporous silicon annealed at 650 °C (Figure S2) (pdf). This material is available free of charge via the Internet at http://pubs.acs.org.

CM0484302